IL NUOVO CIMENTO **39 C** (2016) 330
DOI 10.1393/ncc/i2016-16330-x

COLLOQUIA: La Thuile 2016

QCD Measurements at ATLAS

Z. HUBACEK on behalf of the ATLAS COLLABORATION

Czech Technical University in Prague, Faculty of Nuclear Sciences and Physical Engineering Prague, Czech Republic

received 26 July 2016

Summary. — This paper presents recent QCD related measurements from the ATLAS Experiment at the LHC at CERN. The results on the total inelastic cross-section, charged particle production, jet production, photon production, and W-, Z-bosons productions are briefly summarized. The measurments are performed at different center-of-mass energies $\sqrt{s} = 7, 8$, and 13 TeV. The measured cross-sections are generally found to be in agreement with the expectations from the Standard Model within the estimated uncertainties.

1. – Introduction

Generally, the physics results of proton-proton, proton-lead and lead-lead collisions at the Large Hadron Collider (LHC) [1] can be roughly divided into searches for new unknown physics and precision measurements, which improve our understanding of the so-called Standard Model (SM) of particle physics. This letter describes the latest physics results of the ATLAS Experiment [2] related to the production of primary charged particles, hadronic jets, photons, and W-, Z-bosons. Closely related results of diboson production [3] and four-jet production [4] are also discussed within this proceedings series. The summary of cross-section measurements by the ATLAS Collaboration [5] as a function of center-of-mass energy is shown for selected processes in fig. 1.

A measurement of the inelastic cross-section [6] is performed using scintillator counters mounted in front of the forward calorimeters with $63\,\mu\text{b}^{-1}$ of data from proton-proton collisions at $\sqrt{s} = 13$ TeV. The full inelastic cross-section is determined to be $73.1 \pm 0.9\,(\text{exp.}) \pm 6.6\,(\text{lum.}) \pm 3.8\,(\text{extr.})$ mb, where (exp.) indicates the experimental uncertainties, (lum.) the luminosity uncertainty, and (extr.) the model-dependent uncertainties on the extrapolation from the fiducial region. The measured value as shown in fig. 2 is about one standard deviation below most current theoretical predictions. Inelastic interactions can be divided into nondiffractive or diffractive components, depending

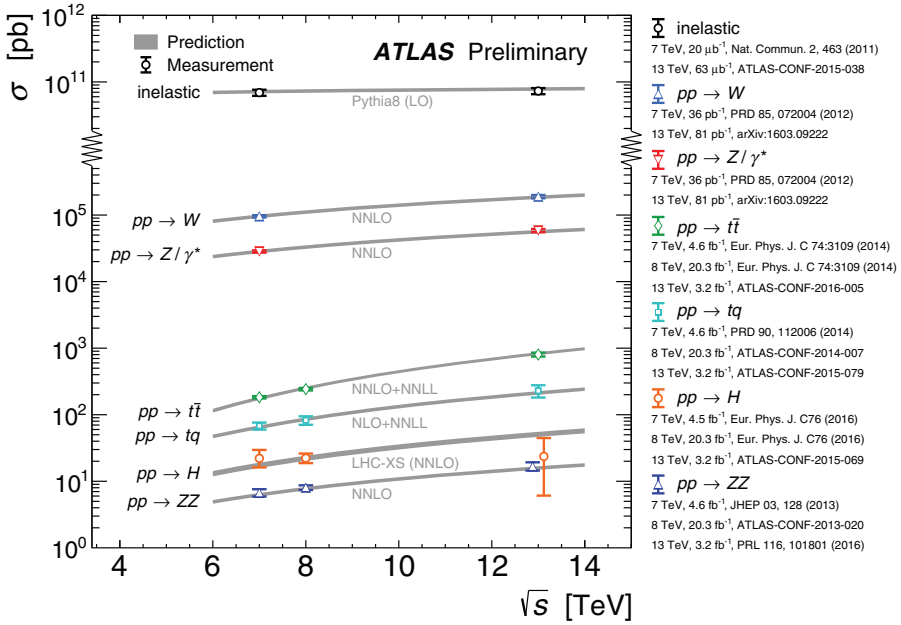

Fig. 1. – Summary of cross-section measurements by ATLAS Collaboration [5] presented as a function of center-of-mass energy $\sqrt{s}$ from 7 to 13 TeV for a few selected processes.

on whether or not one or both protons dissociate in the scattering. Nondiffractive component can be then split into soft and hard part depending on the momentum transfer involved.

2. – Soft QCD results

The strong interaction is described in the framework of quantum chromodynamics (QCD). Inclusive charged-particle measurements in proton-proton collisions provide insight into the strong interaction in the low-energy where perturbative QCD (pQCD) methods cannot be used. Interactions at these momentum transfer scales are typically described by QCD-inspired models implemented in the Monte Carlo (MC) event generators. Primary-charged-particle multiplicities measured at $\sqrt{s} = 13$ TeV [7] as a function of a track transverse momentum, p_{T}, and pseudorapidity, η, in events with at least one charged track with transverse momentum over 500 MeV are shown in fig. 3 overlaid with predictions of four different MC generators. The average primary-charged-particle multiplicities at central pseudorapidity are compared to other existing measurements at different center-of-mass energies in fig. 4 [8].

3. – Jets and photons

At high momentum transfers, collimated sprays of particles, jets, are produced in the hadron-hadron collisions. At these energy scales, the perturbative QCD can be applied and the jet measurements serve as tests of the higher-order calculations, usually corrected for non-perturbative and electroweak effects. Additionally, the cross-section

measurements constrain the parton distribution functions (PDFs) of the proton and can be used to extract the value of the strong coupling constant at high energy scales.

The unfolded inclusive production cross-section of jets [9] reconstructed with the anti-k_{T} jet clustering algorithm with $R = 0.4$ at $\sqrt{s} = 13\,\mathrm{TeV}$ in the central part of the detector with the prediction of next-to-leading order QCD calculation from NLOJET++ using the CT10 PDFs is shown in fig. 5 (left). The dominant systematic uncertainty arises from the jet-energy calibration.

Prompt photon production provides another handle for testing perturbative QCD predictions. Directly produced photons are colorless probes of the hard-scattering process which are directly sensitive to the gluon content of the proton and can thus constrain the PDFs. In the isolated prompt photon cross-section measurement [10], all photons not coming from hadron decays are considered prompt. They include direct photons coming from the hard subprocess and fragmentation photons coming from the fragmentation of a high p_{T} parton. Photons are considered isolated, if the energy carried by partons within a cone centered around the photon is less than a certain criterion ("isolation cut"). The inclusive isolation prompt photon cross-section at $\sqrt{s} = 8\,\mathrm{TeV}$ in four pseudorapidity regions is shown in fig. 5 (right) together with the next-to-leading order prediction from JetPhox using the CT10 PDFs. The total cross-sections are about 20% higher in data than those predicted by JetPhox, but are consistent within the uncertainties.

4. – W- and Z-boson production

The measurement of electroweak vector-boson production [11] tests our understanding of both QCD and electroweak (EW) processes. Theoretical predictions are available up to next-to-next-to-leading order accuracy in QCD and include EW corrections at NLO

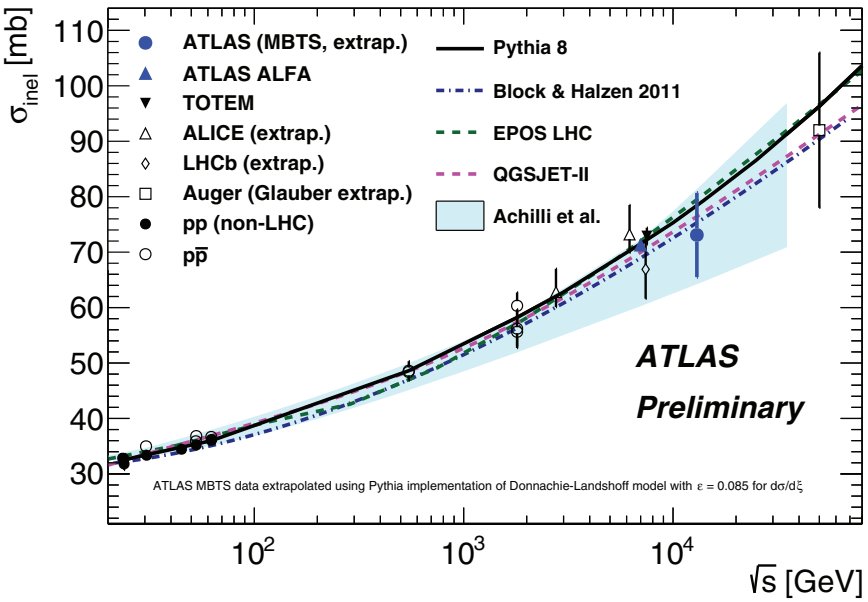

Fig. 2. – The inelastic cross-section measurement with the ATLAS Detector. The new measurement [6] is at $\sqrt{s} = 13\,\mathrm{TeV}$.

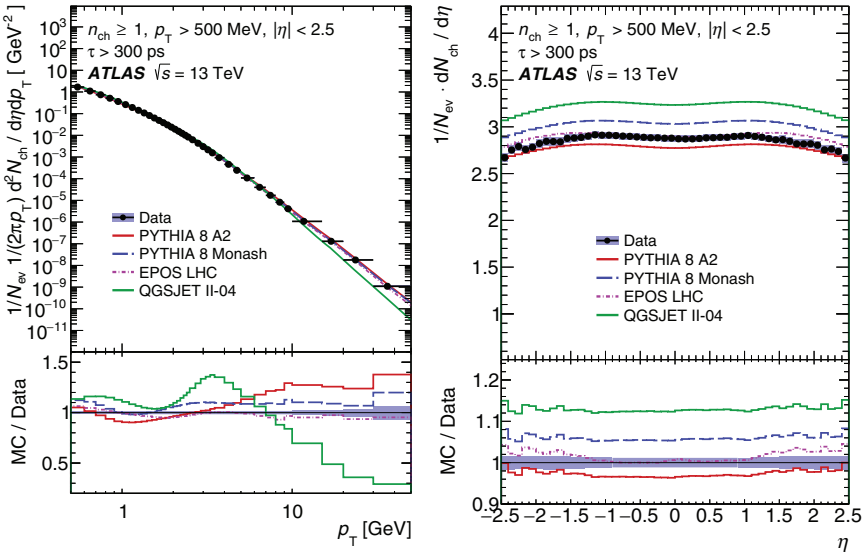

Fig. 3. – Primary-charged-particle multiplicities as a function of transverse momentum, p_{T}, (left) and pseudorapidity, η, (right) in events with $n_{\mathrm{ch}} \geq 1$, $p_{\mathrm{T}} > 500\,\mathrm{MeV}$ and $|\eta| < 2.5$. The dots represent the data and the curves show the predictions from different MC models. Figures from [7].

accuracy. Only the electron and muon decay channels are considered in the following measurements. For the W-boson measurement, the fiducial phase space is defined by the lepton transverse momentum $p_{\mathrm{T}}^{l} > 25\,\mathrm{GeV}$ and lepton pseudorapidity $|\eta_l| < 2.5$, the neutrino transverse momentum $p_{\mathrm{T}}^{\nu} > 25\,\mathrm{GeV}$ and the W-boson transverse mass $m_{\mathrm{T}} > 50\,\mathrm{GeV}$. Similarly, the fiducial phase space for the Z-boson measurement is $p_{\mathrm{T}}^{l} > 25\,\mathrm{GeV}$, $|\eta_l| < 2.5$ and $66 < m_{ll} < 116\,\mathrm{GeV}$, where m_{ll} is the invariant mass of the lepton pair. The dominant background contribution to the W-boson channel are the τ-lepton decay mode of the W-bosons, top-quark production and also the Z-boson dileptonic decay (the W-boson event selection requires exactly one identified electron or muon, but the second lepton from the Z-boson decay could be misidentified in the background process). Similarly, in the Z-boson channel the background is dominated by $t\bar{t}$ production.

The ratios of the predicted to measured fiducial cross-sections for the combined electron and muon channels for both W- and Z-boson production are shown in fig. 6 (left), while the ratios of electron- and muon- channel W- and Z-boson production testing the SM lepton universality are shown in fig. 6 (right).

Events with leptonically decaying Z-boson were also studied in order to improve the modeling of the underlying event [12]. In this measurement at a center-of-mass energy of 7 TeV, several observables sensitive to the underlying event were selected and event properties were analyzed in different ranges of the transverse momentum of the Z-boson candidate $p_{\mathrm{T}}(l^+l^-)$. At small $p_{\mathrm{T}}(l^+l^-)$ values, events are expected to have a low jet activity, while at higher $p_{\mathrm{T}}(l^+l^-)$, one or more hadronic jets are expected to be reasonably described by the pQCD.

The observables were calculated for primary charged particles with transverse momenta $p_{\mathrm{T}} > 0.5\,\mathrm{GeV}$ and pseudorapidities $|\eta| < 2.5$. The following observables were

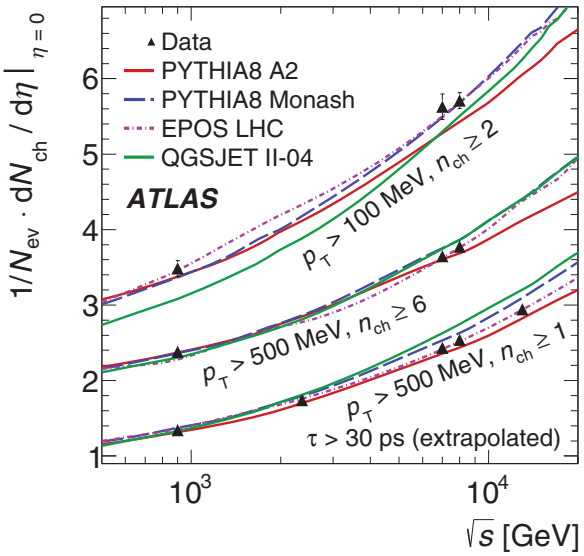

Fig. 4. – The average primary-charged-particle multiplicity per unit of pseudorapidity at $\eta = 0$ as a function of the center-of-mass energy [8]. Results are shown for the phase spaces ($p_{\mathrm{T}} > 500\,\mathrm{MeV}, n_{\mathrm{ch}} \geq 1$), ($p_{\mathrm{T}} > 500\,\mathrm{MeV}, n_{\mathrm{ch}} \geq 6$), and ($p_{\mathrm{T}} > 100\,\mathrm{MeV}, n_{\mathrm{ch}} \geq 2$). The data are compared to various particle-level MC predictions. The results at $\sqrt{s} = 8$ and 13 TeV are extrapolated to include strange baryons. The vertical error bars on the data represent the total uncertainty.

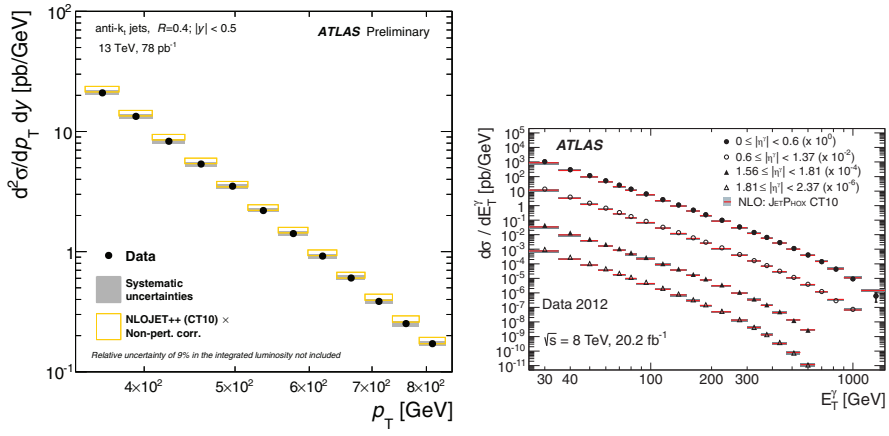

Fig. 5. – Inclusive jet cross-section at 13 TeV [9] (left) and inclusive isolated prompt photon cross-section at 8 TeV [10] (right). Both measurements are compared with the next-to-leading order pQCD predictions using CT10 PDFs.

studied: the charged-particle multiplicity, the scalar sum of transverse momenta of selected charged particles, the beam thrust, the transverse thrust, the sphericity and the $\mathcal{F}$-parameter. Only the charged particle multiplicity and the scalar sum of transverse momenta of selected charged particles are presented in this paper in fig. 7. The distributions are shown for four ranges of the transverse momenta of the Z-boson candidate.

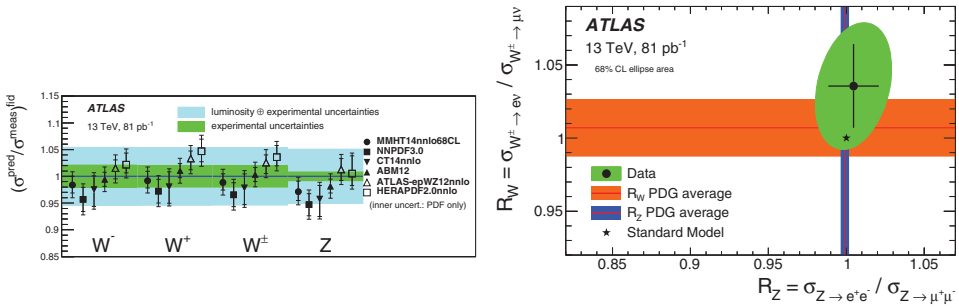

Fig. 6. – Ratio of the predicted to measured fiducial cross-section for the combined electron and muon channels using various PDFs. The inner (outer) band corresponds to the experimental uncertainty without (with) the luminosity uncertainty. The inner error bar of the predictions represents the PDF uncertainty while the outer error bar includes the sum in quadrature of all other systematic uncertainties (left) and ratio of the electron- and muon-channel W- and Z-boson production fiducial cross-sections, compared to the expected values of the SM and previous experimental verifications of lepton universality for on-shell W- and Z-bosons, shown as PDG average bands (right). Figures from [11].

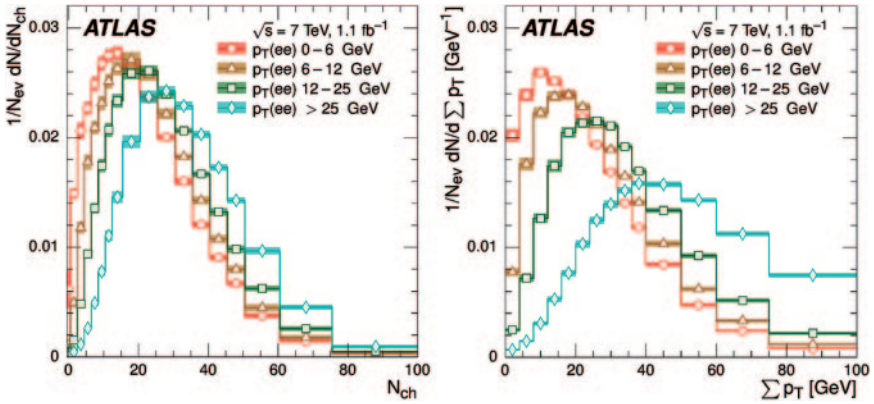

Fig. 7. – Distributions of the event-shape variables from [12]: charged-particle multiplicity N_{ch} (left) and summed transverse momenta Σp_{T} (right) measured in $Z \to e^+e^-$ events for the different ranges of the transverse momentum of the e^+e^- system, $p_{\mathrm{T}}(e^+e^-)$ (open circles: 0–6 GeV, open triangles: 6–12 GeV, open boxes: 12–25 GeV, open diamonds: $\geq$ 25 GeV). N_{ev} denotes the number of events passing the analysis cuts. The bands show the sum in quadrature of the statistical and all systematic uncertainties.

The distributions are compared to different MC generators PYTHIA8, HERWIG7 and SHERPA in fig. 8. Typically, all three generators provide predictions that are in better agreement with the data at high Z-boson transverse momenta than at low Z-boson transverse momenta, and for the observables that are less sensitive to the number of charged particles in the event. The SHERPA event generator shows larger deviations from the measured observables than PYTHIA8 and HERWIG7.

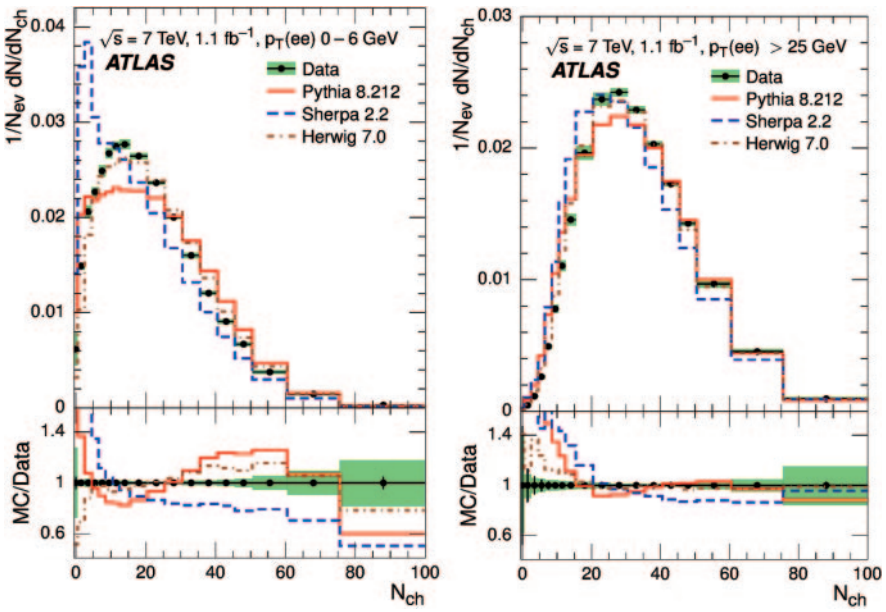

Fig. 8. – Distribution of charged-particle multiplicity, N_{ch}, for $Z \to e^+e^-$ with statistical (error bars) and total systematic (band) uncertainties for the two $p_{\mathrm{T}}(e^+e^-)$ ranges 0–6 GeV (left) and $\geq$ 25 GeV (right) compared to the predictions from the MC generators PYTHIA8 (full line), SHERPA (dashed line), and HERWIG7 (dashed-dotted line). The top plots show the observable and the bottom plots show the ratio of the MC simulation to the data. Figures taken from [12].

5. – Summary and conclusions

This paper has presented recent QCD related measurements from the ATLAS Experiment at different center-of-mass energies of the LHC at CERN. Monte Carlo generators tuned in lower energy regimes describes the latest 13 TeV data well. Generally, a reasonable agreement between theory and experiment is observed. The latest ATLAS public results can be found at `https://twiki.cern.ch/twiki/bin/view/AtlasPublic/StandardModelPublicResults`.

* * *

The author gratefully acknowledges the financial support from the MSMT of the Czech Republic under the Grant No. RVO 68407700.

REFERENCES

[1] EVANS L. and BRYANT P., *JINST*, **3** (2008) S08001.
[2] ATLAS COLLABORATION, *JINST*, **3** (2008) S08003.
[3] SOLODKOV A., these Proceedings.
[4] SACERDOTI S., these Proceedings.
[5] ATLAS COLLABORATION, `https://twiki.cern.ch/twiki/bin/view/AtlasPublic/StandardModelPublicResults#Summary_plots`.
[6] ATLAS COLLABORATION, ATLAS-CONF-2015-038 `https://cds.cern.ch/record/2045064`.

[7] ATLAS Collaboration, CERN-EP-2016-014 https://cds.cern.ch/record/2128621.
[8] ATLAS Collaboration, CERN-EP-2016-020 https://cds.cern.ch/record/2137226.
[9] ATLAS Collaboration, ATLAS-CONF-2015-034 https://cds.cern.ch/record/2038145.
[10] ATLAS Collaboration, CERN-EP-2016-035 https://cds.cern.ch/record/2151982.
[11] ATLAS Collaboration, CERN-EP-2016-069 https://cds.cern.ch/record/2142492.
[12] ATLAS Collaboration, CERN-EP-2016-015 https://cds.cern.ch/record/2134966.